

Radiation tolerance of the LHCb Outer Tracker

D. van Eijk^{a,*}, S. Bachmann^b, Th. Bauer^a, Ch. Färber^b, A. Bien^b, V. Coco^a,
M. Deckenhoff^d, F. Dettori^a, R. Ekelhof^d, E. Gersabeck^b, T.M. Karbach^d, R.
Koopman^a, A. Kozlinskiy^a, Ch. Langenbruch^b, Ch. Linn^b, M. Merk^a, M.
Meissner^b, P. Morawski^e, A. Pellegrino^a, N. Serra^f, P. Seyfert^b, B. Spaan^d, S.
Swientek^d, B. Storaci^a, M. Szczekowski^c, N. Tuning^a, U. Uwer^b, E. Visser^a, D.
Wiedner^b, M. Witek^e

^a*Nikhef, Amsterdam, The Netherlands*

^b*Physikalisches Institut, Heidelberg, Germany*

^c*A. Soltan Institute for Nuclear Studies, Warsaw, Poland*

^d*Technische Universität Dortmund, Germany*

^e*H. Niewodniczanski Institute of Nuclear Physics, Cracow, Poland*

^f*Physik-Institut, Universität Zürich, Switzerland*

Abstract

This paper presents results on the radiation tolerance of the LHCb Outer Tracker (OT) during LHC operation in 2010 and 2011. Modules of the OT have shown to suffer from gain loss after irradiation in the laboratory. Under irradiation at moderate intensities an insulating layer is formed on the anode wire of the OT straw cells. This ageing effect is caused by contamination of the counting gas due to outgassing of the glue used in the construction of the OT modules. Two methods to monitor gain loss in the OT are presented: module scans with radioactive sources and the study of hit efficiency as a function of amplifier threshold. No gain loss is observed after receiving 1.3 fb^{-1} of integrated luminosity corresponding to an integrated charge of 0.055 C/cm in the hottest spot of the detector.

Keywords: Gas detectors, Ageing, Gain loss, Hit efficiency

*Corresponding author

Email address: dveijk@nikhef.nl (D. van Eijk)

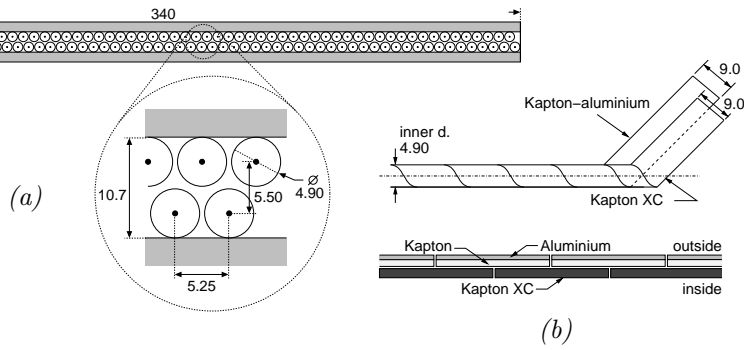


Figure 1: (a) Cross section of an OT module containing 2×64 straw cells. (b) The straws are wound using two foils, kapton-XC and a laminate of kapton and aluminium. All dimensions are given in mm.

16 1. The LHCb Outer Tracker

17 The LHCb experiment is a single arm spectrometer, located at the LHC,
 18 designed to measure CP violation and rare B -decays. The tracking system
 19 consists of silicon strip detectors and straw tube detectors around a large dipole
 20 magnet. The large area behind the magnet is covered by the Outer Tracker
 21 (OT) detector. The OT is a gaseous straw tube detector [1] covering an area of
 22 approximately $5 \times 6 \text{ m}^2$ with 12 detection layers. Every detection layer consists
 23 of a double layer of straw tubes as indicated in Fig.1 (a).

24 The straw tubes are 2.4 m long and 4.9 mm in diameter, and are filled with
 25 the gas mixture Ar/CO₂/O₂ (70%/28.5%/1.5%). A high voltage of 1550 V is
 26 applied to the anode wire, corresponding to a gain of about 5×10^4 [2]. The anode
 27 is made of gold-plated tungsten wire of $25 \mu\text{m}$ diameter, whereas the cathode
 28 consists of an inner foil of electrically conducting carbon doped Kapton-XC¹
 29 and an outer foil consisting of Kapton-XC laminated with a layer of aluminium.
 30 The straws are glued to panels and sealed with sidewalls, resulting in a gas-tight
 31 box enclosing a stand-alone detector module. A sketch of the module layout is
 32 shown in Fig. 1.

¹Kapton® is a polyimide film developed by DuPont.

33 2. Ageing of OT modules

34 2.1. Laboratory tests

35 Laboratory tests with radioactive sources revealed that, despite extensive
36 ageing tests in the R&D phase, the OT modules suffer from gain loss after mod-
37 erate irradiation (i.e. moderate collected charge per unit time), corresponding
38 to approximately 2 nA/cm. Gain losses of 5-25% were observed after 20 hours
39 of irradiation. The origin of the gain loss was traced to an insulating layer
40 containing carbon on the anode wire [3], which is caused by glue outgassing
41 components inside the gas volume [4].

42 The characteristic feature of this ageing phenomenon is a small area of gain
43 loss upstream the radioactive source position. No gain loss is observed down-
44 stream the source, presumably due to the formation of ozone in the high inten-
45 sity region [3]. The contaminated wires have shown to recover the gain after
46 applying a large high voltage of about 1900 V to the anode wire, inducing large
47 dark currents, or by applying a large high voltage of 1860 V while irradiating
48 with a radioactive source [4].

49 2.2. Conditions during LHC operation

50 During most of the 2011 running period, LHCb was operating at an in-
51 stantaneous luminosity of $3.5 \times 10^{32} \text{ cm}^{-2} \text{ s}^{-1}$, which corresponds to a current
52 of 700 nA in the straws located closest to the beam line. The central region
53 of the detector is subject to the largest intensity, corresponding to 14 nA/cm.
54 The LHC delivered a total integrated luminosity of 1.3 fb^{-1} to LHCb in 2011,
55 which translates in a total accumulated dose at the hottest spot of the OT of
56 0.055 C/cm .

57 Two methods to monitor gain loss in the OT will be discussed: scans of the
58 module response with radioactive sources and the study of hit efficiency as a
59 function of amplifier threshold.

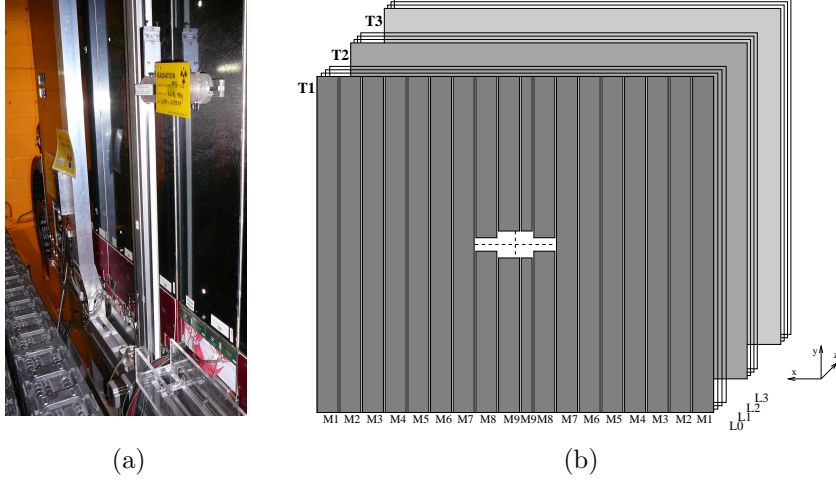


Figure 2: (a) Picture of the scanning setup. The OT modules are visible, as well as the two ^{90}Sr sources in the source holder, which is mounted on the scanning frame. The front-end electronics at the bottom of the scanned module is replaced by a dedicated current meter. (b) Schematic picture of the arrangement of the modules in the LHCb detector.

60 3. Scans with radioactive sources

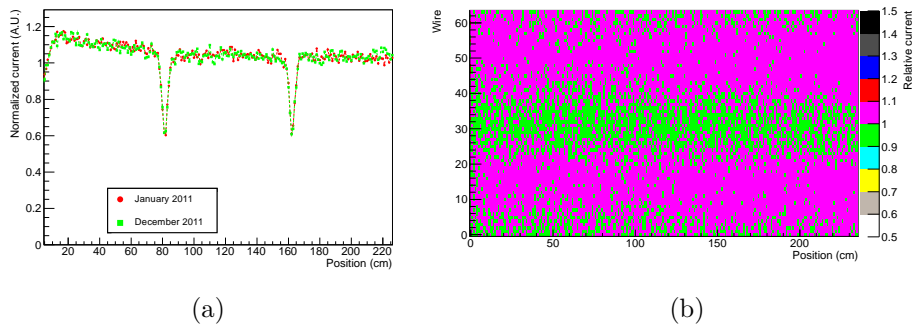
61 3.1. Setup

62 The response of OT modules to radioactive sources before and after LHC
63 operation are performed manually in the LHCb cavern and hence only when
64 the LHC is not in operation. A picture of the setup is shown in Fig. 2 (a). It
65 consists of a frame installed in front of the OT modules accommodating a source
66 holder and a step motor used to move the source holder vertically along the
67 modules. The detector response is determined using two 74 MBq ^{90}Sr sources
68 by measuring the induced current through the wires with a dedicated current
69 meter. The radiation damage in terms of gain loss is quantified by comparing
70 the 2-dimensional current profiles before and after irradiation by LHC operation.
71 The ratio of the currents is expected to be close to unity if no insulating layer
72 is formed on the anode wire.

73 *3.2. Results*

74 The lower half of nine modules, corresponding to a quarter of a detector
 75 layer (see Fig. 2 (b)) were scanned before and after LHC operation in 2011. The
 76 current variation in one wire as a function of the source position is shown in
 77 Fig. 3 (a). The ratio of currents for all 64 wires in one monolayer and for all
 78 positions is shown in Fig. 3 (b). The variations in the relative detector response
 79 of $\pm 10\%$ over the width of the module are attributed to small changes in the
 80 source profile between the two scans.

81 The average change in detector response between January 2011 and De-
 82 cember 2011 amounts to -3% , after correcting for changes in the atmospheric
 83 pressure. This is mainly attributed to the natural decay of ^{90}Sr , which results
 in a lower detector response of about 3% after 1 year.



(a) (b)

Figure 3: *Gain loss scans of an OT module before and after LHC operation in 2011. (a) Normalized current through a wire in January 2011 (green squares) and in December 2011 (red circles). The current drop at positions 80 cm and 160 cm are due to wire locators inside the straw. (b) Relative detector response between January 2011 and December 2011 as a function of wire and position on the module.*

84

85 *3.3. Curing*

86 Before LHC operation, in February 2009, the radiation resistance of the OT
 87 modules was studied by irradiating a module with a single $74\text{ MBq }^{90}\text{Sr}$ source
 88 during 84 hours. The source was collimated with a hole of 6 mm diameter,
 89 resulting in an irradiated area of about $4 \times 4\text{ cm}^2$, with a maximum dose of 0.015

90 C/cm. A maximum gain loss of 38% was observed. The module was scanned
91 again in January 2011 and July 2011 after LHC operation which corresponds to
92 a delivered integrated luminosity of 0.042 fb^{-1} and 0.434 fb^{-1} respectively.

93 The irradiated area is located 1.2 m below the beam axis where the inten-
94 sity induced by the LHC is approximately 0.15 nA/cm . The corresponding to-
95 tal accumulated dose from the LHC in the irradiated area amounts to about
96 0.2 mC/cm . The irradiated area shows a partial recovery in January 2011 and
97 a complete recovery of the gain in July 2011. The current in one wire of this
98 module is shown in Fig. 4. The observed effect shows similarities to the cur-
99 ing effect after applying high voltage [4]. It is unclear whether the underlying
100 microscopic mechanism is related to plasma sputtering of the wire surface or
101 to chemical reactions with radicals such as ozone. An attempt was made to
102 reproduce this curing effect in January 2012, but no gain loss could be provoked
103 after 350 hours of irradiation with a single $74 \text{ MBq } ^{90}\text{Sr}$ source.

104 **4. Amplifier threshold scan**

105 The scans with radioactive sources can only be performed when the LHC is
106 not operational, and only a small selection of modules can be studied. There-
107 fore, a method to monitor possible gain losses in the entire OT and during LHC
108 operation was devised. The readout electronics of the OT is designed to accu-
109 rately determine the time of the hit, but not the charge of the hit. However,
110 by studying the hit efficiency as a function of amplifier threshold during LHC
111 operation, gain variations can be monitored.

112 *4.1. Method*

113 The nominal amplifier threshold is 800 mV , corresponding to a charge collec-
114 tion of approximately 4 fC . The amplifier threshold for a given detection layer
115 is increased in steps from the nominal value of 800 mV to 1450 mV for one OT
116 layer, while all other layers are operated at nominal threshold, in order to prop-
117 erly reconstruct charged particle tracks. This procedure is repeated for all 12
118 layers.

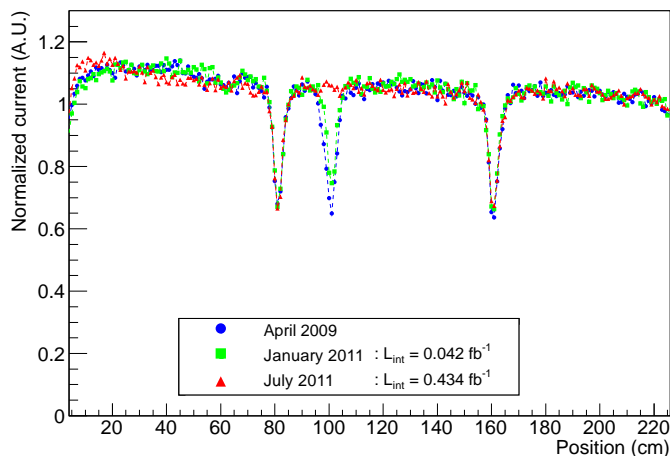


Figure 4: Normalized current as a function of position along a wire in April 2009 (blue circles), January 2011 (green squares) and July 2011 (red triangles). The current loss around position 100 cm in April 2009 is caused by a deliberate irradiation. This gain loss is partly recovered in January 2011 due to LHC operation in 2010 and fully recovered in July 2011 after an additional six months of LHC operation. The current drop at positions 80 cm and 160 cm are due to wire locators in the module.

119 The hit efficiency is determined using tracks with at least 20 hits in the layers
 120 operated at nominal threshold. The hit efficiency is defined as the number of
 121 found hits, divided by the total number of predicted hits, for tracks passing
 122 within 1.25 mm from the wire. The hit efficiency is measured in 85 mm wide bins
 123 of the horizontal coordinate x and 56 mm high bins of the vertical coordinate y .
 124 The bin size in x corresponds to one quarter of the width of an OT module.

125 The hit efficiency as a function of amplifier threshold is shown in Fig. 5. This
 126 characteristic S-curve can be parameterized as:

$$\epsilon_{\text{hit}}(V_{\text{thr}}) = \frac{1}{2}(P + T) - \frac{1}{2}(P - T) \operatorname{erf} \left(\frac{V_{\text{thr}} - H}{\sqrt{2}\sigma} \right) . \quad (1)$$

127 The parameters P and T describe the plateau and the tail of the S-curve re-
 128 spectively. The parameter H is the so-called half-efficiency point, the amplifier
 129 threshold at which the efficiency has dropped to $\frac{1}{2}(P + T)$, while σ accounts for

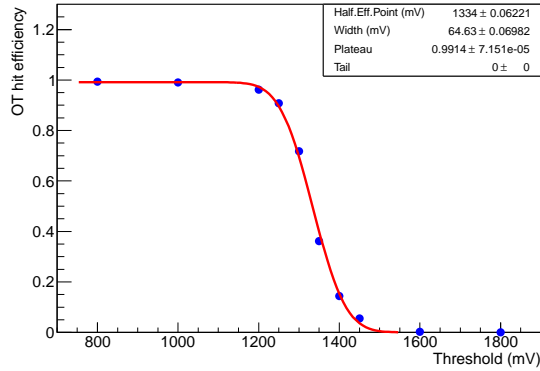


Figure 5: *S-curve fit to threshold scan data taken in October 2011, for layer 0 of the OT (closest to the interaction point). The tail T is fixed to 0, P is found to be 0.99 and H is fitted as 1334 mV. Notice the two points at 1600 mV and 1800 mV are not taken into account in the fit, for fair comparison between all threshold scans taken.*

130 noise.

131 Initially, only eight threshold steps per layer were recorded. Since the hit
 132 efficiency was poorly constrained in the tail, two points at 1600 mV and 1800 mV
 133 were added in the threshold scans recorded from June 2011 onwards. The
 134 hit efficiency at 1600 mV and 1800 mV is observed to be essentially zero and
 135 therefore the tail parameter T is fixed to zero in the S-curve fit. For a fair
 136 comparison between S-curve fits in different threshold scans, only the eight
 137 measurements below 1600 mV are taken into account in the fit. The result of
 138 the fit of Eq. 1 to the hit efficiency as a function of the threshold is shown by
 139 the continuous curve in Fig. 5.

140 Ageing in the Outer Tracker would reduce the charge amplification, due to
 141 the insulating layer on the anode wires. This would lead to an S-curve shifted
 142 to lower values of the amplifier threshold, resulting in a smaller half-efficiency
 143 point. The stability of the half-efficiency point between threshold scans is used
 144 to monitor gain variations in any layer and at any position in x and y . The
 145 threshold scans are performed on a regular basis, such that possible ageing in

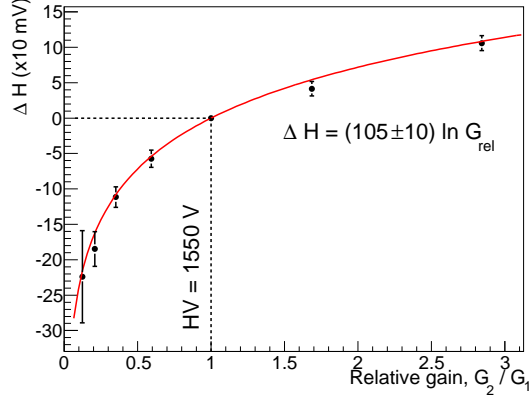


Figure 6: Calibration curve of the shift in half-efficiency point H versus the relative gain. The data points and uncertainties are obtained from the average shift in H of the 64 wires in the module under test.

146 the OT can be detected at an early stage, before the hit efficiency under nominal
 147 conditions is affected.

148 4.2. Gain variations in the OT

149 To relate shifts in half-efficiency point to gain variations, the shift in H as
 150 a function of high voltage was measured [2, 5]. Since the relation between gain
 151 and HV is known, the shift in half-efficiency point $\Delta H = H_2 - H_1$ as a function
 152 of the relative gain $G_{\text{rel}} = \frac{G_2}{G_1}$, was determined, and parameterized as (Fig. 6):

$$G_{\text{rel}} = \exp\left(\frac{\Delta H [\text{mV}]}{105 \text{ mV}}\right) . \quad (2)$$

153 A correction for the atmospheric pressure p is determined from the pulse
 154 height (R) variation as a function of atmospheric pressure shown in Fig. 7, which
 155 is obtained from a dedicated test module which is constantly irradiated by a
 156 radioactive ^{55}Fe source. Since gain is proportional to pulse height the relative
 157 gain is equal to the relative pulse height, which is found to be

$$\frac{\Delta G}{G} = \frac{\Delta R}{R_0} = -5.18 \frac{\Delta p}{p_0} . \quad (3)$$

158

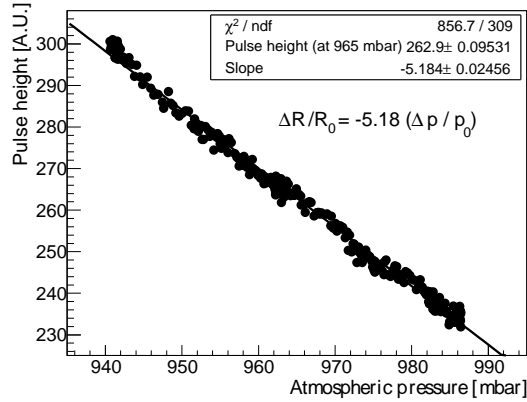


Figure 7: Pulse height R versus atmospheric pressure p as measured on a test module in the

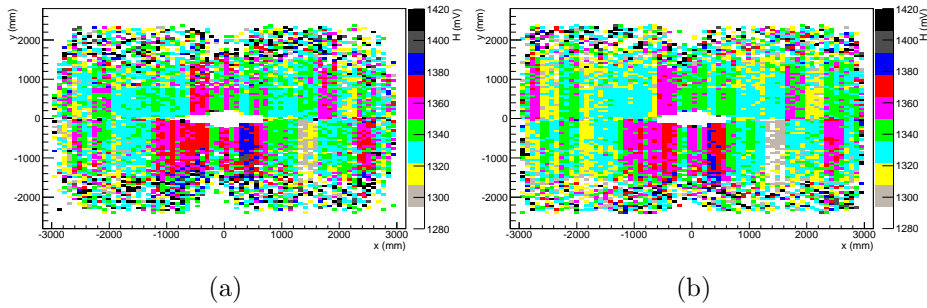


Figure 8: Fitted half-efficiency point H in mV as a function of x and y for OT layer 8 in August 2010 (a) and October 2011 (b). Differences in threshold characteristics of the individual readout electronics units result in the observed module-to-module variations.

159 4.3. Threshold scan results

160 Throughout the 2010 and 2011 run periods, OT threshold scans were per-
 161 formed at regular intervals, corresponding to about 200 pb^{-1} of delivered in-
 162 tegrated luminosity. The duration of one threshold scan is approximately one
 163 hour, collecting about $1.5 \cdot 10^5$ events at each threshold setting.

164 The half-efficiency point H is obtained from a fit of the S-curve in every bin,
 165 as parameterized in Eq. 1, and is shown in bins of x and y in Fig. 8 for two
 166 threshold scans. The first scan is recorded in August 2010, before nominal LHC
 167 operation and the second scan is recorded in October 2011.

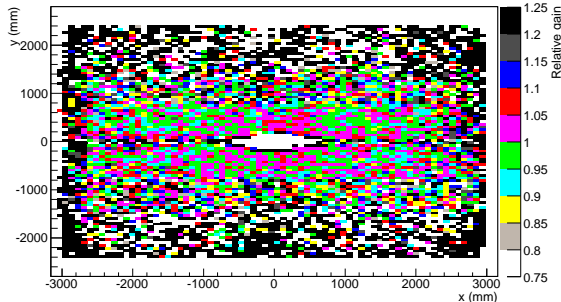


Figure 9: *Pressure-corrected relative gain in bins of x and y for layer 8 of the Outer Tracker between October 2011 and August 2010.*

168 The values for H in every bin from the scans in August 2010 and October
 169 2011 are subtracted, and the relative gain per bin is calculated using the calibra-
 170 tion of Eq. 2 and corrected for the atmospheric pressure. The pressure-corrected
 171 relative gain per bin in x and y is shown in Fig. 9. Apart from bin-to-bin fluctu-
 172 ations, no areas with gain loss (relative gain smaller than 1) are observed. The
 173 statistical accuracy degrades towards the edges of the OT resulting in larger
 174 bin-to-bin fluctuations.

175 To increase sensitivity, the hit efficiency is averaged over regions of the OT
 176 in x and y . Six regions in (x, y) coordinates are studied, averaged over all 12
 177 layers. The inner region is defined as the region within ± 60 cm in both x and y
 178 from the beam pipe and is subject to the highest particle intensity. The outer
 179 region is the region outside ± 60 cm in x and y from the beam pipe. The lower
 180 (upper) region is defined as $y < -60$ cm ($y > 60$ cm). The region closest to the
 181 gas inlet and outlet are defined as $y < -200$ cm and $y > 200$ cm, respectively.

182 As an example, the S-curves for the inner region are shown in Fig. 10. The
 183 shift in fitted half-efficiency point between the two S-curves is $\Delta H = -3.7$ mV,
 184 with a negligible statistical uncertainty, which corresponds to an uncorrected
 185 relative gain of 0.965. Correcting for atmospheric pressure differences during
 186 the two scans, 975.0 hPa and 985.3 hPa in August 2010 and October 2011 re-
 187 spectively, this number changes to 1.021. The pressure-corrected relative gain

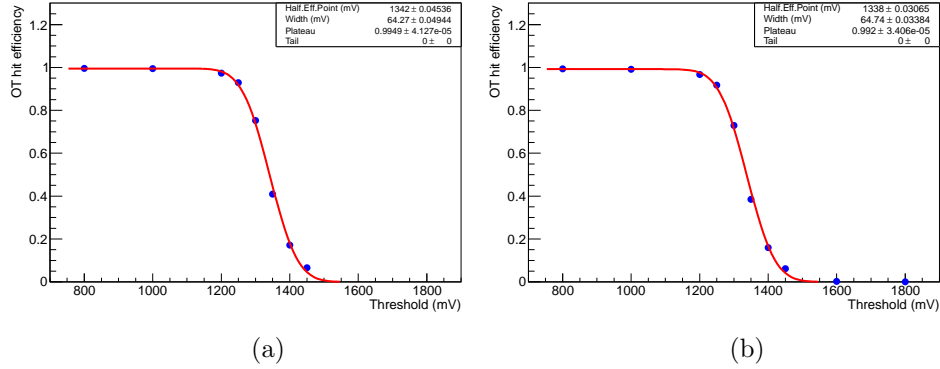


Figure 10: *S*-curve for August 2010 (a) and October 2011 (b) for the inner region, defined as ± 60 cm in x and ± 60 cm in y from the central beam pipe, summed over all OT layers. (Notice that the threshold scan in October 2011 contains two extra data points up to 1800 mV which are not used in the fit for proper comparison between threshold scans.)

188 variation is thus +2.1% for the inner region from August 2010 to October 2011.
 189 The results for the other regions, integrated over the entire OT, are presented
 190 in Table 1, showing a uniform response over the OT surface.

region	coordinates $(x_1, x_2), (y_1, y_2)$ (cm)	pressure-corrected relative gain variation
entire OT	(-300, 300) (-250, 250)	+ 1.3%
inner	(-60, 60) (-60, 60)	+ 2.1%
outer	outside of (-60, 60) (-60, 60)	+ 0.9%
lower	(-300, 300) (60, 250)	- 0.2%
upper	(-300, 300) (-250, -60)	+ 0.2%
gas inlet	(-300, 300) (200, 250)	+ 0.8%
gas outlet	(-300, 300) (-250, -200)	- 2.0%

Table 1: *Relative gain variation between August 2010 and October 2011 for various OT regions summed over all 12 layers, corrected for the change in atmospheric pressure. The various regions are indicated by their coordinates in x and y .*

191 4.4. Systematic Uncertainty

192 To estimate the systematic uncertainty of the method, the fit and the com-
 193 parison procedures have been varied. For every systematic change, the analysis
 194 of the scans in August 2010 and October 2011 is repeated for all regions and the
 195 largest deviation in relative gain variation with respect to the nominal analysis

196 is taken as the systematic uncertainty.

197 The first check is to float the value of the tail parameter T in the fit. A
 198 second check is to constrain $P = 1$, in addition to $T = 0$. Subsequently, the
 199 correction for the atmospheric pressure is varied by a relative $\pm 10\%$. The fitted
 200 parameter of the calibration curve of ΔH versus relative gain was varied by
 201 $\pm 1\sigma$ and the biggest difference is assigned as systematic error. In addition, the
 202 definition of H is changed to the threshold at which the hit efficiency is 0.5
 203 instead of $\frac{1}{2}(P + T)$.

204 The largest difference in relative gain variation per region for each systematic
 205 check is summarized in Table 2. The systematic uncertainties of all checks are
 206 added in quadrature and a total systematic uncertainty of 2.2% is assigned to
 the method.

systematic check	largest difference in relative gain variation per region
T free	+ 1.2%
fix $P = 1$	$\pm 0.0\%$
pressure correction	+ 0.4%
calibration curve $\pm 1\sigma$	+ 0.6% - 0.8%
definition H	-0.4%
double Gaussian fit	+1.5%
total	$\pm 2.2\%$

Table 2: *Changes to the fit and to the scan comparison were applied to estimate the systematic uncertainty. The right column shows the largest deviation in relative gain variation from the nominal analysis in the various regions. The total systematic uncertainty is the quadratic sum.*

207

208 4.5. Time Trend of relative Gain Variation

209 In total, eight full threshold scans have been recorded in 2010 and 2011.
 210 Using the scan from August 2010 as a reference, the relative gain variation as a
 211 function of date and as a function of delivered integrated luminosity, averaged
 212 over the entire OT is shown in Fig. 11 (a) and (b), respectively.

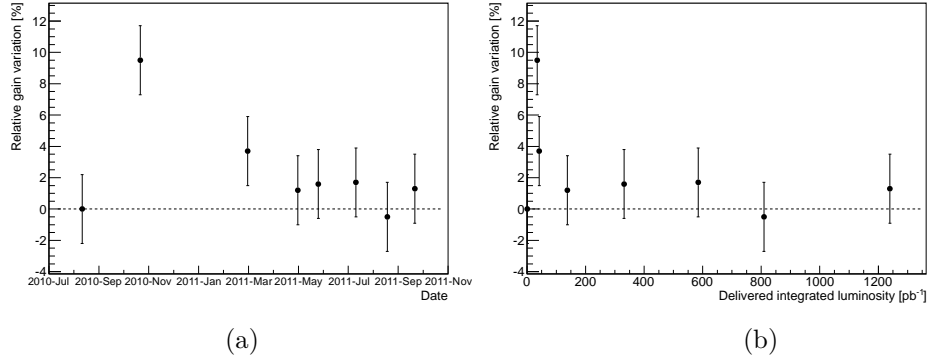


Figure 11: *Relative gain variation averaged over the entire OT compared to August 2010 (indicated by the dashed line) versus date (a) and versus delivered integrated luminosity (b). The error bars indicate the total systematic uncertainty from Table 2 and are fully correlated between the points.*

213 The observed gain increase for the scan in October 2010 with respect to
 214 August 2010 (corresponding to a delivered integrated luminosity of 0.031 fb^{-1})
 215 is not well understood. Overall relative gain variations could be due to variations
 216 in the gas mixture. However, the gas mixture is controlled at a level nominally
 217 better than 0.2%, which would result in a maximum gain variation of 2% and
 218 hence could not explain the observed change in detector response. Relative gain
 219 variations could also be caused by different run conditions. For example, the
 220 average number of pp interactions per bunch crossing is directly correlated to
 221 the event occupancy, which influences the hit efficiency. However, no relation
 222 is found between run conditions and the observed relative gain variations. For
 223 the scans taken after October 2010, no significant time dependence is observed.

224 5. Conclusion

225 Gain loss in the LHCb Outer Tracker is monitored using two techniques:
 226 scanning OT modules with a radioactive source and studying hit efficiency as a
 227 function of amplifier threshold. The first method compares the module response
 228 to ^{90}Sr sources and can only be applied to a small set of modules in periods in
 229 which the LHC is not operational. No significant gain loss is observed in the ^{90}Sr
 230 scans between January 2011 and December 2011. The second technique uses the
 231 OT readout electronics to study hit efficiency as a function of amplifier threshold

232 during LHC operation. Using this method, the relative gain variation averaged
233 over the entire OT between August 2010 and October 2011 is $(+1.3 \pm 2.2)\%$.
234 This indicates that no gain loss is observed in the OT after LHC operation in
235 2010 and 2011.

236 **Acknowledgments**

237 We would like to thank Roel Aaij, Johannes Albrecht and Gerhard Raven for
238 their help on the trigger configuration used in the threshold scans. In addition
239 we would like to thank Rainer Schwemmer and Richard Jacobsson for their help
240 in recording the threshold scans in a proper way and for providing additional
241 information on run conditions during the threshold scans.

242 **References**

- 243 [1] LHCb Coll., 2008, JINST, 3 S08005.
- 244 [2] G. Apeldoorn *et al.*, LHCb-2005-038, 2005.
- 245 [3] S. Bachmann *et al.*, Nucl. Instr. and Meth. A 617 (2010) 202.
- 246 [4] N. Tuning *et al.*, Nucl. Instr. and Meth. A 656 (2011) 45.
- 247 [5] E.L. Visser, CERN-THESIS-2010-094, 2010.